

IFN- γ on day 8 of infection (8, 14, 15). We therefore asked whether IFN- α enhances the stimulation of CD8 T cells isolated from infected mice through the receptor for antigen [the T cell receptor (TCR)]. As shown in Fig. 4B, IFN- α had synergistic effects with the major LCMV immunodominant epitopes recognized through the CD8 TCRs [that is, NP396–404 and GP33–41 (NP, nucleoprotein; GP, glycoprotein)]. Thus, type 1 IFNs do elicit production of IFN- γ by normal cells isolated from mice on day 8 after infection, but they act in concert with CD8 T cell epitopes to drive high levels of IFN- γ release.

Our data indicate that STAT4 activation is a critical intermediary in the induction of mouse IFN- γ by type 1 IFNs. In this capacity, it is rapidly activated and binds to the proximal IFN- γ promoter, and STAT4 deficiency dramatically impairs IFN- α/β -dependent induction of IFN- γ during viral infection. If STAT4 activation by type 1 IFNs is important in the mouse, why was it overlooked and reported not to occur? Previous studies were limited to CD4 T cells (9, 11), genetic constructs in artificial cells (13), use of low concentrations of IFN- α (9, 11, 13), and examination of a mouse strain (9, 11) with reduced STAT4 (26). Although there may be an additional mechanism leading to STAT4 recruitment for activation by type 1 IFNs in humans [that is, a STAT2-dependent pathway (12)], our results indicate that this is not the sole mechanism and that mice and humans do not fundamentally differ in type 1 IFN-mediated regulation of STAT4. Moreover, as STAT1 can have negative effects on responses in both humans and mice (6, 22–25), our observations suggest that major biological consequences of type 1 IFN exposure may be the same in both species if STAT1 effects are dominant. STAT4 activation by type 1 IFNs does not appear to be sufficient for peak IFN- γ induction by CD8 T cells, but this is similar to other stimuli; for example, IL-12 is not sufficient to induce IFN- γ production by resting T cells, because naïve T cells must be activated to up-regulate the IL-12 receptor (2). Likewise, the transcription factor T-bet is an important regulator of IFN- γ production in CD4 T cells, and it too is induced by TCR occupancy but not by type 1 IFNs (27).

Our findings establish a means by which the innate immune response may govern adaptive immunity. More important, however, they provide conceptual insights into mechanisms for plasticity of responses to one cytokine. Together with our earlier work, these findings demonstrate that type 1 IFNs can attenuate or enhance IFN- γ production as a result of differential expression of signaling molecules.

References and Notes

- C. A. Biron et al., *Annu. Rev. Immunol.* **17**, 189 (1999).
- K. M. Murphy et al., *Annu. Rev. Immunol.* **18**, 451 (2000).
- C. A. Biron, *Immunity* **14**, 661 (2001).
- L. P. Cousens, J. S. Orange, H. C. Su, C. A. Biron, *Proc. Natl. Acad. Sci. U.S.A.* **94**, 634 (1997).
- B. L. McRae, R. T. Semnani, M. P. Hayes, G. A. van Seventer, *J. Immunol.* **160**, 4298 (1998).
- K. B. Nguyen et al., *Nature Immunol.* **1**, 70 (2000).
- A. A. Byrnes et al., *Eur. J. Immunol.* **31**, 2026 (2001).
- L. P. Cousens et al., *J. Exp. Med.* **189**, 1315 (1999).
- L. Rogge et al., *J. Immunol.* **161**, 6567 (1998).
- T. Sareneva, S. Matikainen, M. Kurimoto, I. Julkunen, *J. Immunol.* **160**, 6032 (1998).
- C. A. Wenner, M. L. Guler, S. E. Macatonia, A. O'Garra, K. M. Murphy, *J. Immunol.* **156**, 1442 (1996).
- J. D. Farrar, J. D. Smith, T. L. Murphy, K. M. Murphy, *J. Biol. Chem.* **275**, 2693 (2000).
- J. D. Farrar et al., *Nature Immunol.* **1**, 65 (2000).
- K. Murali-Krishna et al., *Immunity* **8**, 177 (1998).
- E. A. Butz, M. J. Bevan, *Immunity* **8**, 167 (1998).
- H. C. Su et al., *J. Immunol.* **160**, 5007 (1998).
- G. C. Pien, R. Salomon, C. A. Biron, W. T. Watford, S. R. Hofmann, A. Morinobu, J. J. O'Shea, unpublished observations.
- Materials and methods are available as supporting material on Science Online.
- J. S. Orange, C. A. Biron, *J. Immunol.* **156**, 1138 (1996).
- J. J. O'Shea, M. Gadina, R. D. Schreiber, *Cell* **109**, S121 (2002).
- X. Xu, Y.-L. Sun, T. Hoey, *Science* **273**, 794 (1996).
- C. V. Ramana et al., *EMBO J.* **19**, 263 (2000).
- Y. Wang, T. R. Wu, S. Cai, T. Welte, Y. E. Chin, *Mol. Cell. Biol.* **20**, 4505 (2000).
- C. V. Ramana et al., *Proc. Natl. Acad. Sci. U.S.A.* **98**, 6674 (2001).
- M. P. Gil et al., *Proc. Natl. Acad. Sci. U.S.A.* **98**, 6680 (2001).
- E. Kuroda, T. Kito, U. Yamashita, *J. Immunol.* **168**, 5477 (2002).
- A. A. Lighvani et al., *Proc. Natl. Acad. Sci. U.S.A.* **98**, 15137 (2001).
- Supported by NIH grant R01-CA41268 (C.A.B.). K.B.N. is supported by a U.S. Department of Education GAANN (Graduate Assistantships in Areas of National Need) training grant, R.S. is supported by NIH F31-GM20760-02, and G.C.P. is supported by a predoctoral fellowship from the Howard Hughes Medical Institute. We thank T. Salazar-Mather, M. Dalod, and W. Montas for their help.

Supporting Online Material

www.sciencemag.org/cgi/content/full/297/5589/2063/DC1

Materials and Methods
Figs. S1 and S2

10 June 2002; accepted 6 August 2002

Evolution of Autoantibody Responses via Somatic Hypermutation Outside of Germinal Centers

Jacqueline William,¹ Chad Euler,¹ Sean Christensen,¹ Mark J. Shlomchik^{1,2*}

Somatically mutated high-affinity autoantibodies are a hallmark of some autoimmune diseases, including systemic lupus erythematosus. It has long been presumed that germinal centers (GCs) are critical in autoantibody production, because they are the only sites currently believed to sustain a high rate of somatic hypermutation. Contrary to this idea, we found that splenic autoreactive B cells in autoimmune MRL.Fas^{lpr} mice proliferated and underwent active somatic hypermutation at the T zone–red pulp border rather than in GCs. Our results implicate this region as an important site for hypermutation and the loss of B cell self-tolerance.

The activation of autoreactive B cells is pivotal for the development of systemic autoimmune diseases, because these lymphocytes secrete pathogenic autoantibodies and promote the activation of pathogenic autoreactive T cells (1). Because affinity-enhancing somatic mutations are prevalent in these autoantibodies, it has long been hypothesized that the GC provides the critical signals for B

cell activation in auto-immune disease. This theory, however, has never been proven, and the steps leading to the production of autoantibodies in systemic autoimmune diseases remain elusive.

The rheumatoid factor (RF) autoantibody response was studied by crossing onto the MRL.Fas^{lpr} (MRL/lpr) lupus-prone mouse strain a transgene (Tg) encoding an immunoglobulin (Ig) Vh (H chain) that is derived from an RF monoclonal autoantibody (AM14) specific for IgG2a of the “a” allotype (IgG2a^a) (2, 3). The resulting mice have a diverse endogenous light chain repertoire along with an increased precursor frequency of an IgG2a^a-specific auto-

¹Department of Laboratory Medicine, ²Section of Immunobiology, Yale University School of Medicine, Box 208035, New Haven, CT 06520–8035, USA.

*To whom correspondence should be addressed. E-mail: mark.shlomchik@yale.edu

REPORTS

antibody that is recreated by the pairing of the AM14 H chain with a rearranged V κ 8 gene product. B cells expressing this autoantibody can be traced using an anti-idiotypic (Id) monoclonal antibody (4-44) raised against the original AM14 hybridoma.

We recently showed that in aged, AM14 H Tg, Fas-deficient (*lpr*), autoimmune-prone mice, numerous RF antibody-secreting cells can be observed (4). Because RF- and other autoantibody-producing B cells in B6/*lpr* and MRL/*lpr* mice are somatically mutated and isotype-switched (5, 6), it was assumed that the autoimmune response of AM14 Id⁺ MRL/*lpr* B cells was generated in GCs. To test this, we stained sections of spleens from a large number of such mice, at a variety of ages, with markers for RF B cells, GCs, and T cells (Fig. 1) (7). Unexpectedly, we observed few RF Id⁺ GCs in these spleens. Instead, RF/Id⁺ B cells were predominantly observed at the T zone-red pulp border (Fig. 1) in areas lacking a follicular dendritic cell (FDC) network (Fig. 1, D and E). Id⁺ cells in these areas were actively proliferating, as indicated by the rapid labeling of a substantial proportion of Id⁺ cells after bromode-

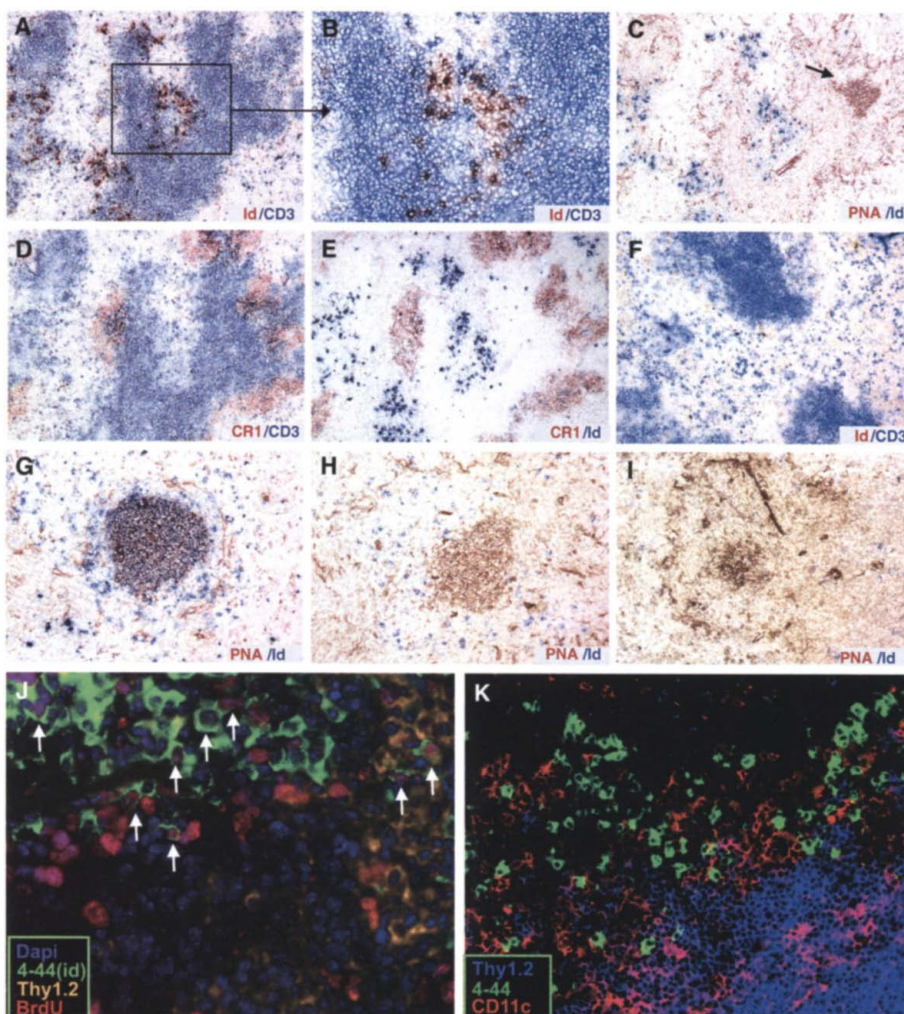
oxyuridine (BrdU) injection (Fig. 1J). As measured by fluorescence-activated cell sorting (FACS) analysis, 15% of splenic RF Id⁺ B cells were labeled within 2 hours of a single injection of BrdU, indicating a high proliferative rate (8). RF Id⁺ cells appeared in clusters ranging from tens to thousands of cells, interdigitated with T cells (Fig. 1, A, B, and K), including large numbers of dark-staining antibody-forming cells (Fig. 1) (9). Furthermore, this process is autoantigen-specific, in that it was never observed in IgH^b congenic mice that lacked the IgG2a^a autoantigen (Fig. 1F), nor was it observed in non-autoimmune-prone mice (4, 10).

Cellular interactions that drive autoreactive B cell proliferation outside of GCs would be substantially different from those within a GC. For example, FDCs, which are thought to regulate B cell proliferation in GCs, are completely absent in the RF⁺ clusters (Fig. 1, D and E). However, CD11c⁺ dendritic cells (DCs) are known to be prevalent at sites similar to those where AM14 B cells proliferate (although rare in GCs) (11). Indeed, staining for anti-Id and CD11c, a DC marker, revealed many DC-RF B cell interactions in

these clusters (Fig. 1K). It is believed that DCs provide unique survival and differentiation signals to B cells and plasmablasts (11).

RF B cell proliferation almost exclusively outside of GCs in the spleen was unexpected, given that autoantibody-secreting B cells from MRL/*lpr* and other autoimmune-prone mice and humans are heavily somatically mutated. To resolve this issue, we hypothesized that a high rate of hypermutation was taking place at these extrafollicular sites of RF B cell proliferation. To test this hypothesis, Id⁺ cells at these sites were microdissected and analyzed (Fig. 2, A and B) by polymerase chain reaction (PCR) amplification using primers specific for genes encoding V κ 8 (12). We created 45 libraries of bacterial clones from independent PCR products. We then sequenced the V κ gene from multiple colonies derived from each library (Table 1 and fig. S1). Nearly all sequences were V κ 8-19 or V κ 8-28 genes joined to J κ 4 and occasionally J κ 5; these two V gene segments are highly homologous to the original V κ 8 gene expressed by the AM14 hybridoma. In most cases, the V genes contained a substantial number of somatic mutations, established by

Fig. 1. RF B cells are at the border of the splenic T zone and the red pulp, not in GCs. [(A) to (E)] Immunohistochemical analysis of adjacent spleen sections from an AM14 MRL/*lpr* mouse. (A and B) Anti-Id staining (red) identifies cells expressing the AM14 H chain and certain V κ 8-family L chains, which together confer RF specificity. CD3 (blue) identifies T cell zones. (C) GCs, identified by PNA (red), are present (arrow) but do not colocalize with Id⁺ areas (blue). (D and E) Id⁺ cells are outside of follicles, identified by monoclonal antibody to complement receptor 1 (CR1), a marker for FDCs. (F) Id⁺ and CD3 staining of the spleen of an AM14 MRL/*lpr* IgH^b mouse. Id⁺ cells do not accumulate in these mice because of the absence of autoantigen. (G) Id⁺ (blue) GCs (red) are easily detectable after immunization of an AM14 H chain MRL/*lpr* IgH^b mouse with IgG2a-containing immune complexes. (H) Identically stained section showing an Id⁻ GC from an alum-immunized MRL/*lpr* IgH^b mouse. (I) An Id⁻ GC arose spontaneously in an H Tg MRL/*lpr* mouse, similar to the GC in (B). As expected, microdissection of approximately 80% of this GC followed by PCR amplification yielded no product. (J) Id⁺ cells in MRL/*lpr* mice proliferate at the T zone-red pulp border. Red, BrdU; green, Id; blue, 4',6'-diamidino-2-phenylindole (DAPI), which stains the nuclei of all cells; and orange, Thy1.2, a T cell marker. Mice were pulsed with BrdU 2 hours before death (8). Proliferating cells will incorporate BrdU in their nuclei. Arrows show some of the BrdU⁺/Id⁺ cells (pink nuclei and green cytoplasm). (K) Spleen section from another AM14 MRL/*lpr* mouse, demonstrating the close interaction of Id⁺ cells (green) with CD11c⁺ DCs (red) and Thy1.2⁺ T cells (blue).



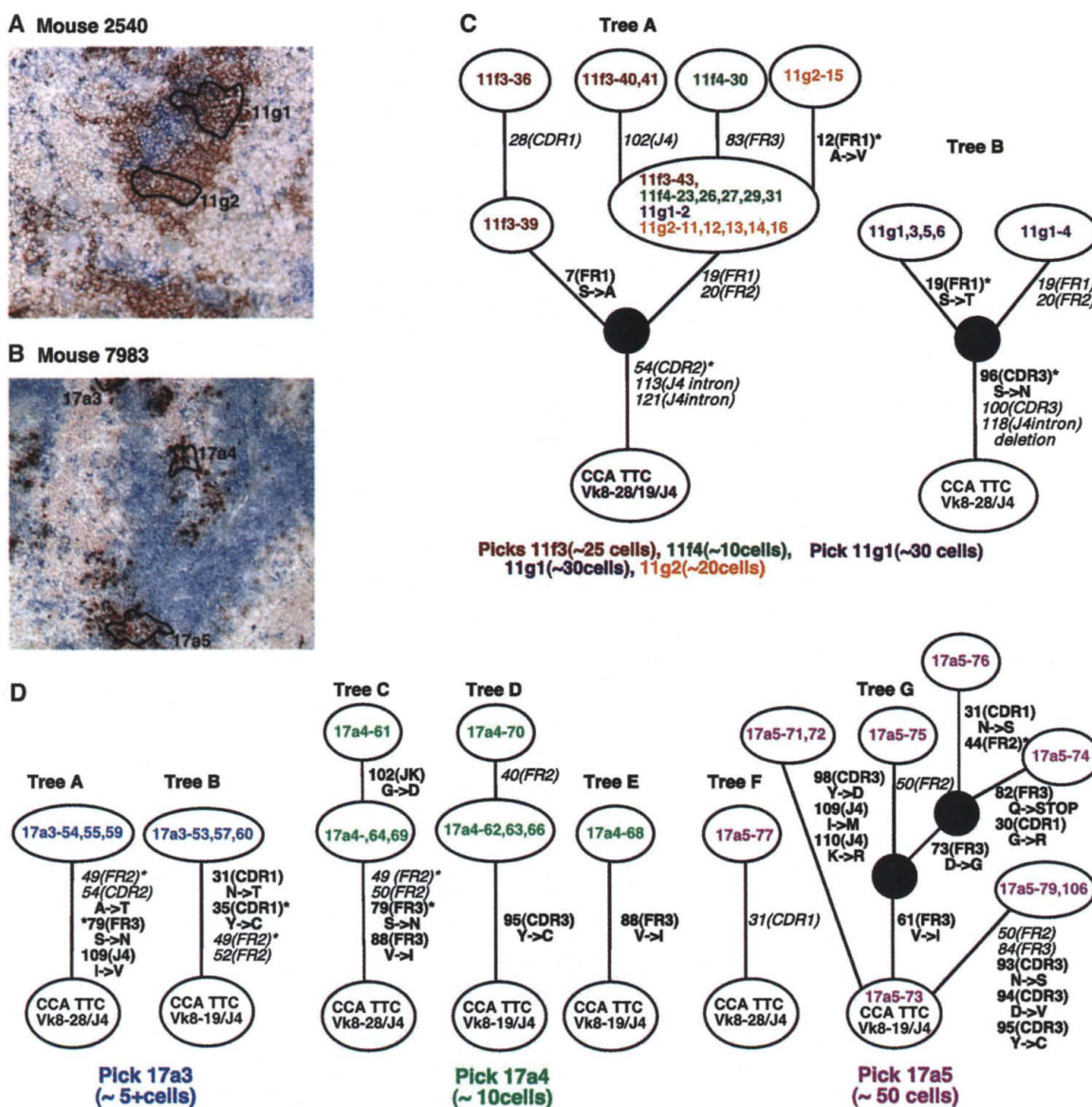
comparison to known germline V and J gene segments (13). Consensus sequences and extensive sequencing of germline DNA (fig. S1) confirmed this conclusion and failed to identify additional germline genes.

In many cases, independent sequences from the same microdissected area differed by one or more mutations, yet shared several other mutations. This hierarchy of shared and unique mutations could be described by genealogical trees, a hallmark of ongoing somatic hypermutation (Fig. 2, C and D). We estimated the light chain mutation rate by mathematical modeling at 0.3 mutations per gene per generation, a rate comparable to that estimated by the same method for hypermutation in GCs (14). Moreover, the pattern of V gene mutations shows clear signs of selection by antigen (table S2).

The unique mutations observed were not the result of mutation elsewhere followed by migration, as sequences from the same or sometimes nearby picks share common mutations and VJ junctions whereas sequences derived from distant sites share a different set of mutations (Table 1 and Fig. 2). Had these unique mutations occurred at distant sites, clonal relatedness would not be confined to local areas. It is still possible that the shared mutations (at the base of the trees) occurred during an initial passage through a GC before further mutation and expansion at the T zone-red pulp border. However, we do not think this is a requirement for mutation outside of GCs, because we have isolated unmutated sequences in the same small picks as mutated sequences (for example, Fig. 2D, tree G).

To confirm the absence of mutating Vκ8 cells in Id⁻ GCs, sections spanning the entire spleen of an H Tg MRL/lpr mouse were stained with peanut agglutinin (PNA) and anti-Id. Of the seven GCs found, all contained few if any visible Id⁺ cells (Fig. 11). The distinction between Id⁻ and Id⁺ GCs is clearly visible histologically (Fig. 1, C and G). Vκ8 PCR amplification of microdissected areas of these GCs yielded a PCR product in only 1 out of 7 GCs, whereas 10 of 10 control Id⁺ GCs were PCR-positive (table S1). The Vκ8 sequences from the lone positive GC of mouse 5281 were unmutated and used a different Jκ segment from the mutated sequences recovered from Id⁺ clusters in nearby and distant T zone-red pulp areas of the same spleen, further arguing against mu-

Fig. 2. Genealogical trees generated from sequences of picks from mice 2540 (A and C) and 7983 (B and D), demonstrating ongoing somatic V region diversification. [(A) and (B)] Blue, CD3; red, Id. Areas outlined in black were microdissected, PCR-amplified, and sequenced. Picks 11g1 and 11g2 had approximately 30 and 20 Id⁺ cells, respectively, and picks 17a3, 17a4, and 17a5 had approximately 5, 10, and 50 Id⁺ cells, respectively. [(C) and (D)] Individual clones were assigned to a particular genealogical tree on the basis of shared and unique mutations. Each open circle represents one or more clones with the same sequence. The numbers of mutated codons are written at the sides of branches. Regions affected are in parentheses. Amino acid changes are written below the codon. Silent mutations are in italics. Mutations that have been seen repeatedly in independent clones, considered hotspots, are indicated by asterisks. Inferred intermediates in clonal evolution are represented by dark circles. Picks 11f3 and 11f4 (C) were taken from the same cluster as 11g1 and 11g2, in an adjacent section. All clones from this same region have a unique germline sequence resembling a combination of the Vκ8-19 and Vκ8-28 gene loci (see fig. S1). Circles at the base of trees represent germline sequences.



Sequences for mouse 7983 were isolated from picks taken from three different foci on the same T cell zone, yet each focus has a unique set of mutations. A mutation in tree G produces a stop codon.

REPORTS

tation in GCs followed by migration to an Id⁺ site. In some spleens that have ongoing mutation, no GCs of any type are seen (Table 1 and fig. S2). Somatic hypermutation out-

side of GCs in RF Tg Fas-deficient mice differs fundamentally from mutation that has been documented in severely immunodeficient mice defective in GC formation. For

example, in CD40L- and LT α -deficient mice, the mutation process occurs at unidentified sites (perhaps residual GCs), and mutations themselves are infrequent (15, 16). However, AM14 Tg B cells undergo a high rate of somatic hypermutation at a clearly defined histologic site. Furthermore, Fas-deficient mice are immunocompetent and do have normal GC formation after immunization (17, 18), although this can be reduced in older mice.

The facts that Fas-deficient mice can form GCs that support normal somatic hypermutation (17, 18) and that RF B cells are clearly capable of entering GCs (Fig. 1, G and H) (9) raise the question of why RF B cell mutation in the spleen occurs in extrafollicular sites. Most likely, there is an unusually long duration of RF B cell proliferation at the T zone-red pulp border in AM14 Tg MRL/lpr mice (9). We therefore propose that somatic hypermutation is induced whenever B cells are stimulated to undergo a substantial number of cell cycles under conditions where antigen- and T cell-derived signals required for mutation are present (19). This hypothesis would explain why mutation occurs in GCs, in vitro under appropriate conditions (19), and at extrafollicular sites in chronic autoimmune responses.

RF B cells may persist in MRL/lpr mice because of lack of Fas-mediated apoptosis. However, during foreign protein immune responses, apoptosis and involution of proliferative foci at the T zone-red pulp border occur normally in Fas-deficient mice (20). Therefore, we favor the idea that chronic exposure to antigen as observed in AM14 spleens (fig. S3) and/or the form of the antigen perpetuates the response at the T zone-red pulp border. Autoantibodies commonly target macromolecules with repeating determinants, such as immune complexes and chromatin, that could provide a sustained and strong antigen signal. Another unique facet of the RF response is the potential of chromatin-containing immune complexes to co-stimulate AM14 RF B cells via Toll-like receptor 9, as recently demonstrated in vitro by Leadbetter *et al.* (21). Such signals could lead to altered localization and/or differentiation of somatic hypermutating B cells. Leadbetter *et al.* have suggested that the ability to co-signal through Toll-like receptors may be a unifying feature of dominant autoantigens (21). If so, then mutation outside of GCs may be common in antibody responses.

Because somatic mutations can create autoreactive B cells from innocuous ones, mechanisms that censor autoreactive mutants are likely to be important in the GC (22-24). These protective mechanisms may be the reason why mutation is normally restricted to the GC. However, when the antigenic stimulus is chronic and the antigens involved may stim-

Table 1. Summary of all microdissections and sequences along with the distribution of mutations in those sequences. A PCR product was retrieved in ~75% of microdissections. Sequences recovered from eight mice were grouped by pick and assigned to a lettered genealogical tree. Mutations were classified into three categories based on their positions in these trees. Identical sequences in a pick were conservatively treated as one clone, instead of as the products of multiple cells, and were assigned to one unique sequence. Trunk mutations from picks that have no branches in the genealogy are in bold (for example, Fig. 2D, pick 17a3).

Mouse	Pick	Tree*	Cells picked	Total sequences†	Total unique sequences‡	Mutations per unique sequence	Trunk§ mutations per unique sequence	Branch mutations per unique sequence	
								Shared	Unique¶
2205	5a2	A	10	3	3	13.7	12.0	0.0	1.7
	5a3	A	10	5	4	13.3	12.0	0.0	1.3
	5a5	B	15	8	6	2.2	1.0	0.0	1.2
	b1	C	30	7	3#	1.0	0.0	0.0	1.0
	5b3	D	25	6	1#	0.0	0.0	0.0	0.0
	5b4	E	15	1	1	2.0	2.0	0.0	0.0
		F		4	1	2.0	2.0	0.0	0.0
	5c1	G	50	3	3	3.0	2.0	0.0	1.0
		H		5	3#	1.4	0.0	0.7	0.7
	5c2	I	30	4	3	4.4	2.0	0.7	1.7
		J		2	2	2.5	2.0	0.0	0.5
	5f1	K	50	3	1	1.0	1.0	0.0	0.0
		L		5	1	2.0	2.0	0.0	0.0
		M		2	1	2.0	2.0	0.0	0.0
		5f2	K	50	3	2	1.5	1.0	0.0
2540	11f3	A	25	5	4	5.0	3.0	1.5	0.5
	11f4	A	10	6	2	5.5	3.0	2.0	0.5
	11g1	A	30	1	1	5.0	3.0	2.0	0.0
		B		5	2	4.5	3.0	0.0	1.5
	11g2	A	20	6	2	5.5	3.0	2.0	0.5
	11h1	C	5	5	1#	0.0	0.0	0.0	0.0
4270		D		4	2	4.5	4.0	0.0	0.5
	10c1	A	5	8	1	10.0	10.0	0.0	0.0
	10j1	B	10	6	1	3.0	3.0	0.0	0.0
	10j2	C	20	6	3	6.6	4.0	1.3	1.3
	10j4	D	3	2	1#	0.0	0.0	0.0	0.0
4641		E		3	1#	0.0	0.0	0.0	0.0
	12a2	A	5	7	2	2.5	2.0	0.0	0.5
	12b1	B	12	5	2	1.5	1.0	0.0	0.5
		C		2	1	2.0	2.0	0.0	0.0
	12c1	D	10	6	1	2.0	2.0	0.0	0.0
	12c2	E	6	7	2	5.5	5.0	0.0	0.5
	12d2	F	50	5	4#	2.5	0.0	0.5	2.0
		G		4	2#	0.5	0.0	0.0	0.5
		H		1	1#	0.0	0.0	0.0	0.0
		12e1	I	20	5	2	13.5	13.0	0.0
5205	2e2	J	5	6	1	13.0	13.0	0.0	0.0
	13a1	A	15	7	1	4.0	4.0	0.0	0.0
	13d1	B	20	8	1#	0.0	0.0	0.0	0.0
5281	13d3	C	12	8	1	5.0	5.0	0.0	0.0
	14a1	A	10	6	3	10.7	10.0	0.0	0.7
7976	14a3	A	10	5	1	10.0	10.0	0.0	0.0
	14c1	B	30	7	4	5.3	1.0	3.5	0.8
	14c2	C	10	5	3#	2.3	0.0	2.0	0.3
	16b3	A	15	6	3	4.4	2.0	0.7	1.7
		B		2	2	2.5	2.0	0.0	0.5
	16b5	C	10	8	1	4.0	4.0	0.0	0.0
	16c1	D	50	5	1	1.0	1.0	0.0	0.0
16c2	E	15	7	3#	0.7	0.0	0.0	0.7	
	F		8	2	1.5	1.0	0.0	0.5	
	16c3	G	10	4	2	9.5	9.0	0.0	0.5
		H		1	1	6.0	6.0	0.0	0.0
	16d1	I	20	8	3	6.7	6.0	0.0	0.7
	16d2	J	20	7	2	3.5	3.0	0.0	0.5
	16e2	K	10	7	1	5.0	5.0	0.0	0.0

Table 1 (continued).

Mouse	Pick	Tree*	Cells picked	Total sequences†	Total unique sequences‡	Mutations per unique sequence	Trunk§ mutations per unique sequence	Branch mutations per unique sequence	
								Shared	Unique¶
7983	17a3	A	5	3	1	4.0	4.0	0.0	0.0
		B		3	1	4.0	4.0	0.0	0.0
	17a4	C	10	3	2	4.5	4.0	0.0	0.5
		D		4	2	1.5	1.0	0.0	0.5
		E		1	1	1.0	1.0	0.0	0.0
	17a5	F	50	1	1	1.0	1.0	0.0	0.0
		G		8	6#	3.0	0.0	0.8	2.2
	17b1	H	10	2	1	6.0	6.0	0.0	0.0
		I		5	1	5.0	5.0	0.0	0.0
	Total			853	305	125			
Weighted average						4.3	3.2	0.4	0.7

*Genealogical tree to which sequences in a pick are assigned. Equivalent letters in an individual mouse are part of the same tree. †All sequences derived from a pick. ‡Total number of different sequences in a pick. §Mutations shared by all of the clones on a tree and preceding branch mutations. ||Mutations that are seen in multiple sequences of a pick. ¶Mutations that occur in only one unique sequence of a pick. #Trees containing one or more germline sequences. All mutations present in such trees are counted as branch mutations.

ulate through unique pathways, B cells may mutate elsewhere (25) and thereby escape the mechanisms that normally censor autoreactive B cells in the GC environment.

References and Notes

- M. J. Shlomchik, J. Craft, M. J. Mamula, *Nature Rev. Immunol.* **1**, 147 (2001).
- M. J. Shlomchik, D. Zharhary, T. Saunders, S. Camper, M. Weigert, *Int. Immunol.* **5**, 1329 (1993).
- L. G. Hannum, D. Ni, A. M. Haberman, M. G. Weigert, M. J. Shlomchik, *J. Exp. Med.* **184**, 1269 (1996).
- H. Wang, M. J. Shlomchik, *J. Exp. Med.* **190**, 639 (1999).

- M. J. Shlomchik, A. Marshak-Rothstein, C. B. Wolfowicz, T. L. Rothstein, M. G. Weigert, *Nature* **328**, 805 (1987).
- M. J. Shlomchik *et al.*, *J. Exp. Med.* **171**, 265 (1990).
- Materials and methods are available as supporting material on Science Online.
- J. William, C. Euler, S. Christensen, M. J. Shlomchik, unpublished observations.
- J. William, C. Euler, M. J. Shlomchik, in preparation.
- J. William, C. Euler, S. Christensen, M. J. Shlomchik, in preparation.
- C. Garcia De Vinuesa *et al.*, *Eur. J. Immunol.* **29**, 3712 (1999).
- Cells were captured with a glass micropipette attached to an Eppendorf Transferman micromanipula-

tor. Vκ8/J4 rearranged sequences were amplified by nested PCR using Pfu Turbo (Stratagene). Amplified DNA was cloned and further amplified by picking transformed colonies directly into a PCR amplification reaction using M13 external primers. The PCR product was then purified and sequenced with a T3 primer. See supporting online material for details.

- R. Thiebe *et al.*, *Eur. J. Immunol.* **29**, 2072 (1999).
- S. Kleinstein, Y. Louzoun, unpublished data.
- S. Weller *et al.*, *Proc. Natl. Acad. Sci. U.S.A.* **98**, 1166 (2001).
- M. Matsumoto *et al.*, *Nature* **382**, 462 (1996).
- K. G. Smith, G. J. Nossal, D. M. Tarlinton, *Proc. Natl. Acad. Sci. U.S.A.* **92**, 11628 (1995).
- Y. Takahashi, H. Ohta, T. Takemori, *Immunity* **14**, 181 (2001).
- E. Kallberg, S. Jainandunsing, D. Gray, T. Leanderson, *Science* **271**, 1285 (1996).
- D. Watanabe, T. Suda, S. Nagata, *Int. Immunol.* **7**, 1949 (1995).
- E. A. Leadbetter *et al.*, *Nature* **416**, 603 (2002).
- K. M. Shokat, C. C. Goodnow, *Nature* **375**, 334 (1995).
- S. Han *et al.*, *J. Immunol.* **155**, 556 (1995).
- B. Pulendran, K. G. C. Smith, G. J. V. Nossal, *J. Immunol.* **155**, 1141 (1995).
- A. E. Schroder, A. Greiner, C. Seyfert, C. Berek, *Proc. Natl. Acad. Sci. U.S.A.* **93**, 221 (1996).
- We thank A. Haberman, J. Craft, M. Nussenzweig, and M. Weigert for critical reading of the manuscript; A. Rothstein for useful discussions; S. Kleinstein and Y. Louzoun for collaboration on mutation rate calculations and sharing their unpublished results; and W. DeLage for expert animal care. Supported by grant P01-A36529 from NIH.

Supporting Online Material

www.sciencemag.org/cgi/content/full/297/5589/2066/DC1

Materials and Methods

Figs. S1 to S3

Tables S1 and S2

Reference S1

14 May 2002; accepted 10 July 2002

Coordinated Reactivation of Distributed Memory Traces in Primate Neocortex

K. L. Hoffman and B. L. McNaughton

Conversion of new memories into a lasting form may involve the gradual refinement and linking together of neural representations stored widely throughout neocortex. This consolidation process may require coordinated reactivation of distributed components of memory traces while the cortex is "offline," i.e., not engaged in processing external stimuli. Simultaneous neural ensemble recordings from four sites in the macaque neocortex revealed such coordinated reactivation. In motor, somatosensory, and parietal cortex (but not prefrontal cortex), the behaviorally induced correlation structure and temporal patterning of neural ensembles within and between regions were preserved, confirming a major tenet of the trace-reactivation theory of memory consolidation.

Our ability to recall detailed memories, even from the distant past, suggests that we have a robust, high-capacity neural system for storing memories. Yet, in the minutes to days

after an event, memory for that event is susceptible to disruption. This period of lability may be a consequence of the way memory traces are stored throughout the cortex.

Marr (1) was perhaps the first to suggest how a sparsely connected hierarchical network such as the cortex may be capable of high-capacity, detailed representation, with the caveat that the final memory trace is not

made entirely "on-the-fly" (2–5). Instead, after an event occurs, a top-down cascade of neural activity may ensue. Event-related activity in cells from higher level regions of cortex (e.g., hippocampus and related associational structures) may elicit activity in cells from lower level regions that were also active during the event. Through repeated coactivation, these lower level ensembles may create the connections necessary to encode the memory trace efficiently and to sustain it, or some approximation of it, independently of top-down input. This "trace-reactivation" theory is one of several theories that explain the protracted period of time required for memory consolidation and why cortical association areas, such as the hippocampus, are necessary during such consolidation periods. Two critical predictions follow from this theory: (i) Patterns of neural ensemble activity expressed during an experience should be spontaneously reactivated during subsequent periods of behavioral inactivity; and (ii) the distributed components of the reactivated memory trace should appear concurrently within the relevant cortical sites.

Consistent with the former prediction, neural ensembles in the rat hippocampus and

Division of Neural Systems, Memory, and Aging, University of Arizona, Tucson, AZ 85724, USA.
*To whom correspondence should be addressed. E-mail: bruce@nsma.arizona.edu